The JPL Serpentine Robot: a 12 DOF System for Inspection

Eric Pal jug, Timothy Ohm, and Samad Hayati
Jet Propulsion Laboratory
4800 Oak Grove Drive
Pasadena, CA 91109-8099

Abstract

The *Serpentine Robot is a* prototype hyper-redundant (snake-like) manipulator system developed at the Jet Propulsion Laboratory. It is designed to navigate and perform tasks in obstructed and constrained environments in which conventional 6DOF manipulators cannot similarly function. 'I'his paper describes the Serpentine Robot mechanical design, a low level inverse kinematic algorithm for the joint assembly, a brief synopsis of control development to date, and the applications of this technology.

1 Introduction

The Jet Propulsion Laboratory has been studying the utility of telerobotics toward inspection tasks in space, and for the space station in particular [6]. Inspection tasks can include scanning the surface for flaws and impact, damage, temperature anomalies, stress cracks, and gas leaks. However, not all surfaces (or inspection areas in general) are easily accessible With a telerobotic manipulator. The 8 DOF arm used within the JPL Remote Surface Inspection Laboratory, although quite dextrous, has limitations in its ability to reach around and through complex and obstructed environments.

Serpentine robot technology [1, 2, 3] is designed to be able to navigate these types of congested environments by incorporating many degrees of freedom (DOF) into the design. This technology often involves novel mechanical designs and control approaches. This paper focuses on the J]'], Serpentine Robot mechanical design and low level control, thus high level control schemes are only briefly discussed.

This paper is organized as follows: The next section describes the robot system design and lists its overall specifications. Section 3 describes the design details Of the serpentine robot 2-DOF joint and the kinematic methods that can be used to control the motors, including an inverse kinematic algorithm for this system.

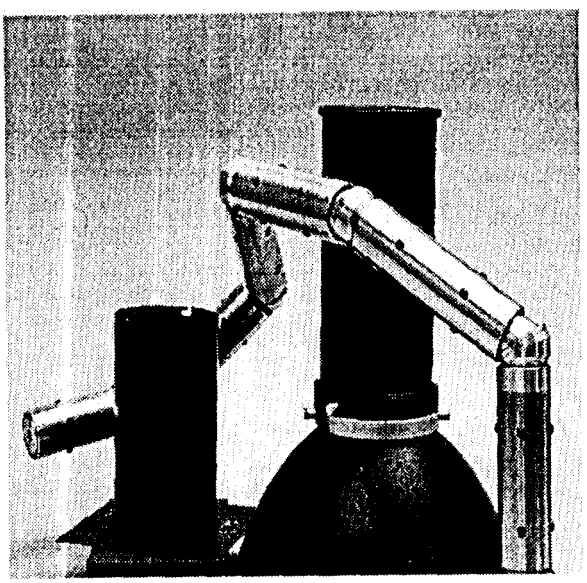

Figure 1: The Serpentine Robot in an obstructed workspace.

Section 4 briefly outlines how high level control methods can be applied to control the redundant joints of the serpentine robot. Section 5 describes inspection applications for the serpentine robots. Finally, the paper ends with conclusions and acknowledgements in Section 6.

2 Serpentine Robot System Design

The desired application of the Serpentine Robot imposes design requirements uncommon to conventional robots. It must be compact but *very* capable of navigating obstructed worksites. The following features are desired:

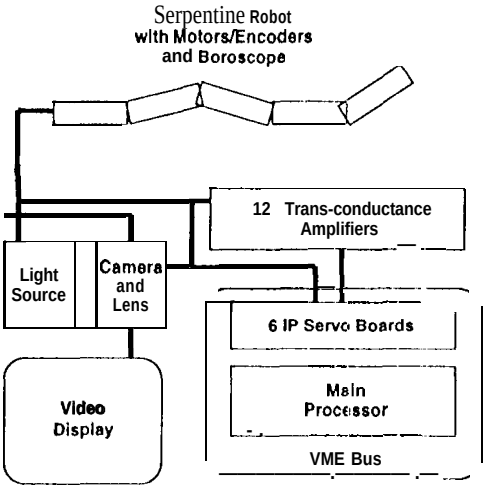

Figure 3: The control system hardware architecture.

3 Mechanical Design of the Serpentine Robot Joint

The key to accomplishing the performance requirements is the mechanical design of the serpentine joint. It was developed from a design originally by Ikeda and Takanashi [5] of the NEC Corporation. This original design put forth the the concept of an *active* universal joint. The Jet l'repulsion Laboratory innovative implementation of this joint places the universal joint structure within the gear-head and bearing assembly, thereby enabling the gear-head and bearing system to handle larger loads and to accommodate a center pass through for wires and fiber optics.

The kinematics of the joint is developed below, an algorithm to solve the inverse kinematics is presented, and the forward differential kinematics arc discussed to provide more insight.

3.1 Joint Kinematics

Figure 4 depicts a kinematic diagram of the joint which is then redrawn as two separate set of frames, the internal universal joint is shown in Figure 5 and the external gear-lmaring-gear system is shown in Figure 6. Consider frame A and frame B, which have co-located origins at the intersection of the axes of the universal joint, where A is attached to the base and B is attached to the output link (see Figure 5). The internal structure of the universal joint will only permit a yaw and pitch motion between frames A and B. Thus, the relationship of frame B with respect to A is written in Equation 2 as a homogeneous transform that is a function of a (yaw) rotation α shout, the neg-

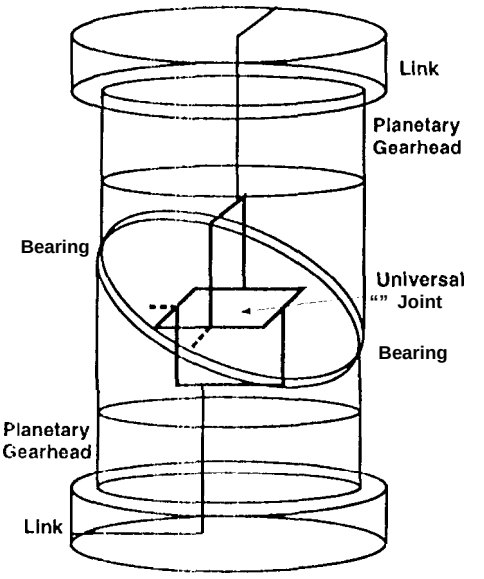

Figure 4: The kinematic diagram of the Serpentine Robot joint, showing the internal universal joint and the external gearhead-bearing-gearhead system.

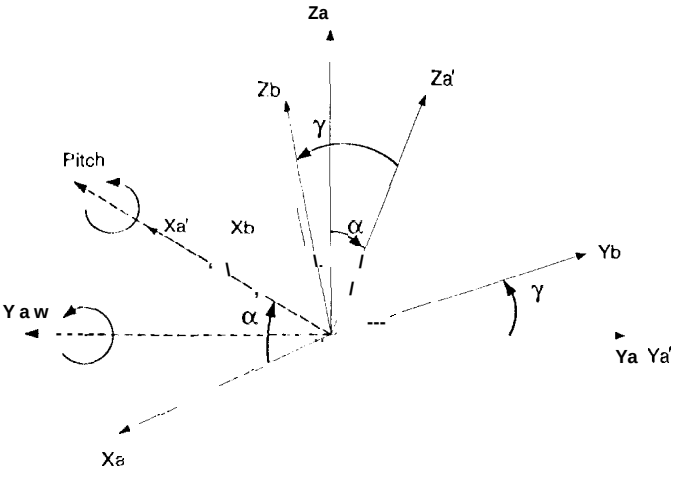

Figure 5: The kinemat ic frames of the universal joint in terms of yaw and pitch angles.

$$
{}^{3}_{0}T(\theta_1,\theta_2,\theta_3) =
$$

$$
\begin{bmatrix}
c_1c_2c_3 - K_c^2c_2s_1s_3 - K_s^2s_1s_3 - K_c s_2 s_{13} & -(K_c^2c_2c_3s_1) - C, K_s^2 s_1 - K_c c_1 c_3 s_2 - c_1c_2s_3 + K_c s_1 s_2 s_3 & -(K_c K_s s_1) + K_c c_2 K_s s_1 + c_1 K_s s_2 & 0 \\
c_2c_3s_1 + K_c c_{13} s_2 + K_c^2 c_1 c_2 s_3 + c_1 K_s^2 s_3 & K_c^2 c_1 c_2 c_3 + c_1 c_3 K_s^2 - c_2 s_1 s_3 - K_c s_2 s_{13} & K_c c_1 K_s - K_c c_1 c_2 K_s + K_s s_1 s_2 & 0 \\
-(c_3 K_s s_2) + K_c K_s s_3 - K_c c_2 K_s s_3 & K_c c_3 K_s - K_c c_2 c_3 K_s + K_s s_2 s_3 & K_c^2 + c_2 K_s^2 & 0 \\
0 & 0 & 0 & 1
\end{bmatrix} \quad (1)
$$

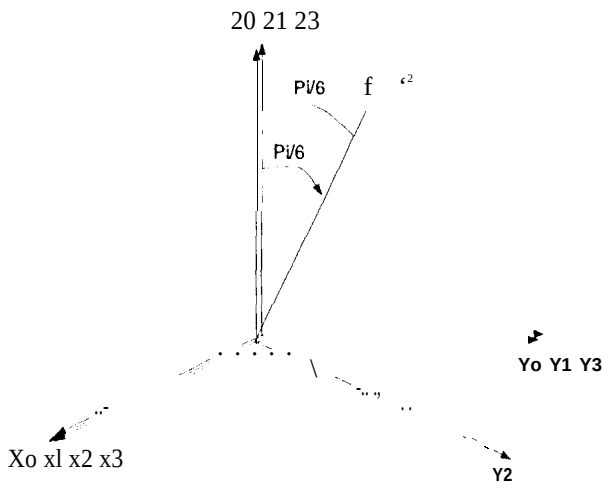

Figure 6: The kinematic frames of the gearhead-hearing-gearhead system in terms of the motor 1, bearing, and motor 2 angles.

ative Y_a axis to form the intermediate frame A' and then a (pitch) rotation 7 shout the $X_{a'}$ axis of the inter'mediate frame A'.

$$
{}^{A}_{B}T(\alpha,\gamma) = \begin{bmatrix} c_\alpha & -s_\gamma s_\alpha & -c_\gamma s_\alpha & 0 \\ 0 & c_\gamma & -s_\gamma & 0 \\ s_\alpha & c_\alpha s_\gamma & c_\alpha c_\gamma & 0 \\ 0 & 0 & 0 & 1 \end{bmatrix} \quad (2)
$$

In this notation, $c_n = \cos(n)$ and $s_n = \sin(n)$, where $n = \alpha$ or γ. Note that there is no twist (roll) between the two frames, an important feature of the original design. In this implementation, it also will prevent any pass through wires or fiber optic bundles from being torsionally stressed.

In Figure 6, the gear-head and hearing assembly schematic is depicted. Each end of the joint is composed of planetary gear-head. Without the structure of the universal joint,, these heads are free to move with respect to each other upon a bearing which lies on a plane that is tilted 30 degrees from the perpendicular planes of each gear-head axes of rotation. In the schematic of Figure 6, the frames 0, 1, 2, and 3 have co-located origins at the intersection of the axes of rotation of the top and bottom gear-heads as well as the bearing in between them. Frame O is the base fram e and each of the other frames are attached to one of the DOF's of this system: frame 1 is attached to the lower gear-head output, frame 2 is attached to the output of the bearing, and frame 3 is attached to the upper gear-hcad (input). The Z axis of each of these frames points along the axis of rotation: Z_1 for the lower gear-head, Z_2 for the bearing, and Z_3 for the upper gear-head. The relationship of frame 3 with respect to O is written in Equation 1 as a homogeneous transform that is a function of a rotation θ_1 shout, the Z_1 axis, a rotation θ_2 about the Z_2, and a rotation θ_3 ahout the 2, axis. In this notation, $c_n = \cos(\theta_n)$ and $S_n = \sin(\theta_n)$ for $n = 1,2,3$ and $C_{13} = \cos(\theta_1 + \theta_3)$ and $s_{13} = \sin(\theta_1 + \theta_3)$, while $K_c = \cos(\frac{\pi}{6})$ and $K_s = \sin(\frac{\pi}{6})$.

Note that θ_1 and θ_3 are determined hy motor one and two, respectively, and θ_2 is not explicitly controlled. However, θ_2 (the hearing angle) is none the less constrained by the structure provided by the universal joint which prevents a twist between the base and upper frame.

Thus, the two t.ra.rlsfor'ins, ${}^{A}_{B}T$ and ${}^{0}_{3}T$, arc equivalent transformations for this joint, assembly. The subsequent link is able to yaw and pitch ± 60 degrees with respect to the previous link. A singularity exists when the pitch and yaw are zero, where the mechanism is only capable of an instantaneous yaw motion and cannot perform an instantaneous pitch motion.

3.2 Joint Inverse Kinematics

The inverse kinematics takes advantage of the fact that

$$ {}^{A}_{B}T(\alpha,\gamma) = {}^{0}_{3}T(\theta_1,\theta_2,\theta_3) $$

and that the yaw and pitch angles (α, 7) arc given. The angle θ_2 is solved for by equating the third row, third column elements of the above transforms. In general, two solutions are found $(\pm\theta_2)$. If $\alpha = 7 = 0$, no solution exists as the joint is in a singular configuration. Otherwise, $\theta_1(\theta_3)$ is solved for by equating elements 1,3 and 2,3 (3,1 and 3,'2) of these matrices for both values of θ_2. Finally, during real-time operation, one of the solution triplets $(\theta_1,\theta_2,\theta_3)$ is chosen based on previous locations of these variables in order to preserve continuity.

3.3 Joint Differential Kinematics

It is interesting to examine the differential kinematics of the joint in terms of the spherical coordinate system of ϕ and θ, where ϕ is the angle measured from the pole of the sphere (z0 in the case of Figure 6) and θ is measured with respect to an axis normal to the equator of the sphere (X_0 in Figure 6). Constant angular velocities of the motors can produce orthogonal motions of the output link based on the direction of rotation. The motor velocities ω_1 about Z_1 and ω_3 about Z_3 produce a velocity $\dot{\phi}$ when subtracted and they produce a velocity $\dot{\theta}$ when added, as given below:

$$ \dot{\phi} = K_1(\omega_1 - \omega_2) \quad (3) $$

$$ \dot{\theta} = K_2(\omega_1 + \omega_2) \quad (4) $$

where K_i account, for the gear ratios.

4 Control Approaches

The high level control algorithms for serpentine manipulators must resolve the redundancy issue in order to perform the task. Approaches to this problem include [3, 4]. The concepts of damped least squares and configuration control [7] are incorporated in [8]. This algorithm assumes the tip of the serpentine robot obtains a valid trajectory (either from *a priori* information, on-line sensor feedback, or operator input) and attempts to have each subsequent link *follow the leader*. ~'bus, the mechanism travels *snake-like* through congested environments.

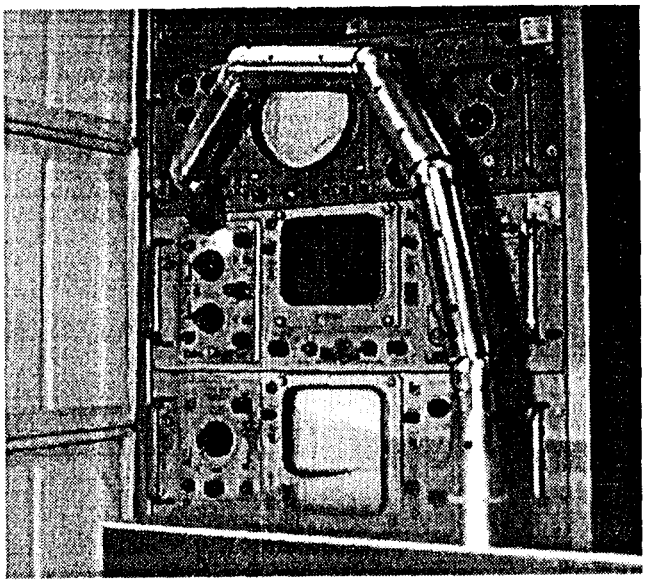

Figure 7: The Serpentine Robot in the Charlotte/Space Hab mock-up.

5 inspection Applications

The Serpentine Robot is being tested in two inspection applications. In one case, a genuinely hyper-redundant implementation by adopting a macro-micro configuration in which the Serpentine robot, is held at the end of the much larger, 7 DOF Robotics Research Corporation Model K1207 manipulator [4, 8]. By including the additional linear translation of the base of the macro-manipulator, this system will contain 20 DOF. The RRC arm has been used to investigate telerobotic inspection tasks for space station, and with the additional capabilities of the Serpentine Robot, the system will be able to better access obstructed and constrained areas of truss structures for insertion.

The second application involves the Serpentine Robot integrated with a mock-up of the Charlotte IVA Robot by McDonnell Douglas and it interacts with a mock-up of the Space Shuttle Space Hab Laboratory. The Charlotte robot is a cable suspended mechanism that can move about the entire open area Of the Space Hab, but it is unable to inspect areas that arc recessed within the Space Hab test racks. With this design of the Serpentine Robot, these recessed areas can be inspected by a remote operator. Figure 7 shows the serpentine robot within this mock-up.

6 Conclusions

The JPL Serpentine Robot is designed for inspection tasks in constrained and obstructed environments (on Earth and in space). The 2-DOF joint, implementation is well suited for these applications since it not only provides kinematic flexibility, but it also has better load capabilites and contains a center pass- through for convenient packaging of electonic wires and fiber optic cables. The kinematic solution of this joint involves analyzing the system of a universal joint in parallel with a 3 DOF gearhead-bearing-gearhead assembly. The system is currently being evaluated two inspection applications at the Jet I'repulsion Laboratory.

7 Acknowledgements

The work described in this document was performed at the Jet Propulsion Laboratory, California Institute of Technology, under contract with the National Aeronautics and Space Administration.

References

[1] S. Hirose *et. al.* Design and Control of a Mobile Robot with an Articulated Body. In *The International Journal of Robotics Research,* Vol '3, No. 2, April 1990.

[2] K. Asano *et. al.* Multijoint Inspection Robot. In *The IEEE Transactions on Idustrial Electronics,* Vol IE-30, No. 3, 1'383.

[3] G. Chirikjian and J. Burdick *et. al.* Kinematics of Hyper-redundant Robot Locomotion with Applications to Grasping. In *The* Proceedings *of the IEEE International Conference on Robotics and Automation, 1991.*

[4] *T.* Lee and T. Ohm and S. Hayati. Design, Control, and Applications of a Serpentine Robot, Part 1: Design, Fabrication and Control. In *The Proceedings of the International Symposium on Robotics and Manufacturing,* 1994.

[5] H. Ikeda and N. Takanashi. Joint Assembly Moveable Like a Human Arm. United States Patent Number 4,683,406, July 1987.

[6] S. Hayati and B. Balaram *et. al.* Remote Surface Inspection, In *Robotics and Autonomous Systems,* Vol. 11, No. 1, 1993.

[7] H. Seraji. Configuration Control of Redundant Manipulators: Theory and Implementaiton. In *IEEE Transactions 071 Robotics and Automation,* Vol. 5, No. 4, 1989.

[8] R. Colbaugh and K. Glass and H. Seraji. Control of a Serpentine Robot for Inspection Tasks. In *The Proceedings of the International* Symposium *on Robotics and Manufacturing,* 1994.

[9] Technology 80, Inc. Model 28/29 Users Guide. Revised August 1994.